J. Phys. B: At. Mol. Opt. Phys. 27 (1994) 1981–1992. Printed in the UK

Spin-resolved photoelectron spectroscopy of HBr in the resonance region of electron autoionization

M Salzmann, N Böwering, H-W Klausing, R Kuntze and U Heinzmann
Fakultät für Physik, Universität Bielefeld, 33501, Bielefeld, Germany
and
Fritz-Haber Institut der MPG, 14195 Berlin, Germany

Received 8 December 1993, in final form 21 February 1994

Abstract. The spin polarization parameters A and ξ, the cross section σ and the angular distribution parameter β in outer shell photoemission from HBr were measured in the resonance region of electronic autoionization between the $HBr^+ X\,^2\Pi$ and $HBr^+ A\,^2\Sigma^+$ thresholds using photoelectron spectroscopy with circularly polarized synchrotron radiation. In this region the photoelectron spectra display pronounced vibrational excitation of the $X\,^2\Pi$ final ionic states. The energy dependence of the dynamical parameters is strongly influenced by electronic autoionization and predissociation of vibrational progressions of Rydberg states. The data for σ and A are combined to obtain cross sections for the outgoing partial waves. A comparison of the experimental results with *ab initio* MQDT calculations of Lefebvre-Brion indicates that predissociation is more important than theoretically predicted.

1. Introduction

In vacuum ultraviolet photoionization of the outer valence shell of molecules, autoionization resonances can have pronounced effects on photoionization and photoabsorption spectra. In such spectra, the intensity contributions resulting from direct ionization of the neutral ground state to the final ionic state are often strongly altered by indirect ionization via intermediate autoionizing resonances. Further modifications of the spectra can arise from predissociation of the intermediate states. In the case of photoionization of the hydrogen halides, the energy region between the first and second ionization thresholds is affected by both electronic autoionization and predissociation. The influence of these processes and competition between them was the subject of several investigations in recent years for the molecules HCl (Lefebvre-Brion *et al* 1988, Lefebvre-Brion and Keller 1989), HBr (Lefebvre-Brion *et al* 1989) and HI (Böwring *et al* 1992a, b). Since the photoionization process is determined by complex matrix elements not only the photoionization cross section σ but also the angular distribution parameter β and the spin polarization parameters of the photoelectrons are influenced by the presence of resonant states. These parameters each depend on the transition amplitudes and phases in a different way (see, e.g., Raseev *et al* 1987); therefore, more detailed information on the photoionization dynamics can be obtained from measurements of the energy dependence of several parameters in the energy region of interest. In this paper, we present experimental results on the photon energy dependence of σ, β, the spin polarization parameters A and ξ, and determine partial cross section contributions

0953-4075/94/101981+12$19.50

σ^{λ} for the $X\,^2\Pi_{3/2}(v=0)$ and $X\,^2\Pi_{1/2}(v=0)$ final ionic states of HBr^+ in the electronic autoionization region between the $X\,^2\Pi$ ground state and the $A\,^2\Sigma^+$ excited state of HBr^+. Furthermore, we give a comparison of the experimental results for σ, A and β with *ab initio* MQDT calculations by Lefebvre-Brion (reported by Lefebvre-Brion *et al* 1989) for the $X\,^2\Pi_{1/2}(v=0)$ final ionic state.

The non-bonding $(4p\pi)^4$ and the bonding $(4p\sigma)^2$ orbitals form the closed outer shells of the ground state of the hydrogen halide HBr (Ballard 1978). Photoionization of the $p\pi$ electron changes the dissociation energy and the equilibrium bond length of the molecule only very slightly, whereas the photoionization of a $p\sigma$ electron causes a substantial increase of the equilibrium bond length of the ion (Ballard 1978). Consequently, as a result of the Franck–Condon principle (FCP), for the neutral ground state HBr $X\,^1\Sigma^+(v=0)$ no substantial vibrational excitation appears by direct ionization of an electron from the non-bonding $4p\pi$ orbital, whereas the removal of an electron from the $4p\sigma$ orbital leads to vibrationally excited levels of the $A\,^2\Sigma^+$ final ionic state. This is reflected in the photoelectron spectra for photon energies above the $A\,^2\Sigma^+$ threshold, where only the $(v=0)$-components of the HBr^+ $X\,^2\Pi_{3/2}$ and $X\,^2\Pi_{1/2}$ states appear, whereas for the first excited state HBr^+ $A\,^2\Sigma^+$ a progression of vibrational levels can be observed (Delwiche *et al* 1972/73). The vibrational structure of the photoelectron spectra of the $A\,^2\Sigma^+$ state for HBr^+ is perturbed by predissociation (Adam *et al* 1992) arising via spin–orbit coupling between the $A\,^2\Sigma^+$ state and the repulsive $^4\Sigma^-$, $^2\Sigma^-$ and $^4\Pi$ ionic states (Lempka *et al* 1968) leading to a broadening of highly vibrationally excited levels. For illustration, some of the most important neutral, ionic and electronically excited states of HBr discussed in this paper are represented in figure 1 by potential energy curves. A more detailed figure of potential curves for the HBr^+ ionic states may be found in the recent paper of Yencha *et al* (1991).

For photon energies *below* the $A\,^2\Sigma^+$ threshold vibrational excitation of the HBr^+ $X\,^2\Pi$ final ionic states occurs as a consequence of resonant photoionization processes involving vibrationally excited Rydberg states with an $A\,^2\Sigma^+$ ion core (see, e.g. the

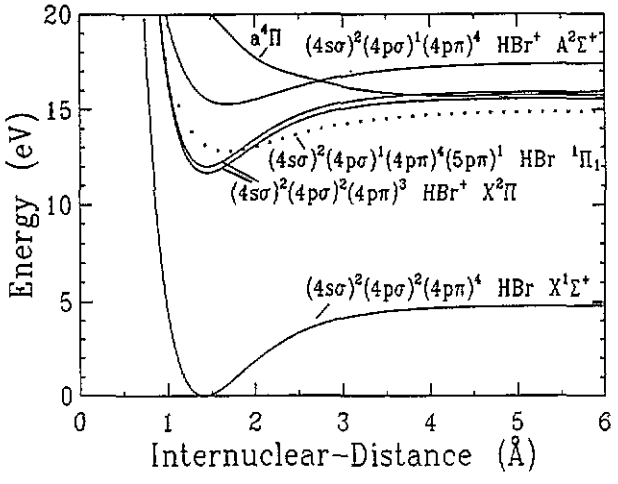

Figure 1. Morse potential curves for the $^1\Sigma^+$ ground state of HBr, the $^2\Pi$ ground and $^2\Sigma^+$ excited state of the HBr^+ ion, one of the repulsive ionic states ($^4\Pi$) (solid lines), as well as one Rydberg state of HBr ($^1\Pi_1$, dotted line). The constants used for the Morse potential curves are taken from Huber and Herzberg (1979) and Banichevich *et al* (1992).

dotted curve in figure 1). These Rydberg states are populated by photoexcitation of an electron from the molecular $4p\sigma$ orbital and may decay by autoionization giving rise to vibrationally excited states of $HBr^+ X\,^2\Pi$. The corresponding process was found recently for the HI molecule (Böwering *et al* 1992a), where photoelectron spectra with vibrationally excited $x\,^2\Pi$ final ionic states were observed. Previous investigations for HBr have demonstrated that above the $^2\Pi_{1/2}$ threshold of the ion the photoionization process is dominated by electronic autoionization and predissociation caused by Rydberg series converging to the excited ionic state $A\,^2\Sigma^+$ (Terwilliger and Smith 1974, 1975, Lefebvre-Brion *et al* 1989). The most intense autoionizing Rydberg states of HBr are the $(4p\sigma)^1(4p\pi)^4(5p\sigma)^1\,^1\Sigma^+$, $(4p\sigma)^1(4p\pi)^4(5p\pi)^1\,^1\Pi$ and $(4p\sigma)^1(4p\pi)^4(4d\pi)^1/(5d\pi)^1\,^1\Pi$ resonances (Lefebvre-Brion *et al* 1989). The vibrational levels of these autoionizing Rydberg resonances are partially predissociated due to curve crossings with repulsive states belonging to Rydberg series converging to the $^4\Sigma^-$, $^2\Sigma^-$ and $^4\Pi$ ionic states, namely the $^3\Sigma_1^+$ and $^3\Pi_0$ states (Lefebvre-Brion *et al* 1989, Lefebvre-Brion and Keller 1989). The characterization of the Rydberg resonances follows Lefebvre-Brion *et al* (1989).

The final states, with non-zero transition moment from the ground state have $^1\Sigma^+$ and $^1\Pi$ symmetry. For the $(p\pi)^{-1}$ ionization three continuum states $(^2\Pi, \varepsilon l\pi)^1\Sigma^+$, $(^2\Pi, \varepsilon l\sigma)^1\Pi$ and $(^2\Pi, \varepsilon l\delta)^1\Pi$ exist for the $HBr^+\,^2\Pi$ final ionic state with outgoing partial waves $\varepsilon l\lambda$ with $l=0, 1, 2, \ldots$ and $\lambda=\sigma, \pi, \delta$ (l is the photoelectron angular momentum and λ its projection on the internuclear axis).

The analysis of the resonance region of HBr was discussed in a previous publication where the first experimental results for the A parameter were compared with the calculation (Lefebvre-Brion *et al* 1989). In this report we provide more detailed dynamical information for the energy region from 12.7–14.7 eV, since now more extensive measurements not only for the parameter A but also for the parameters σ, β and ξ have been completed. The combined information contained in these dynamical parameters, in particular in the parameters σ and A (which depend only on the transition amplitudes and not on the phases) allows a further partitioning of the various partial cross section contributions in this resonance region to be achieved.

2. Experimental details

The photoelectron spin polarization and intensity measurements were carried out at the storage ring BESSY using circularly polarized synchrotron radiation at the 6.5 m NIM (Schäfers *et al* 1986) with an apparatus described elsewhere (Heckenkamp *et al* 1986). Briefly, the monochromatic light (bandwidth $\Delta\lambda_{FWHM}=0.4$ nm, with an additional uncertainty in the accuracy of the photon energy scale of $\Delta\lambda=0.05$ nm for the spin polarization measurements, and $\Delta\lambda_{FWHM}=0.17$ nm for the intensity measurements, degree of circular polarization: 92%) was crossed by an effusive beam of HBr molecules (purity 98%). The emitted photoelectrons at the emission angle Θ (angular resolution $\Delta\Theta=5°$) were analysed by a rotatable hemispherical spectrometer (Jost 1979) (energy resolution $\Delta E_{FWHM}=120$ meV for the spin polarization and $\Delta E_{FWHM}=75$ meV for the intensity measurements). The photoelectrons were accelerated to 100 keV and analysed with respect to their spin polarization in a Mott detector (Sherman function $S=-0.23$). The spin polarization components $A(\Theta)$ (component parallel to the photon momentum) and $P_\perp(\Theta)$ (component perpendicular to the reaction plane given by the momenta of

the photon and photoelectron) are described by the energy dependent parameters A, α, ξ and β according to the following equations (Heckenkamp *et al* 1984):

$$P_{\perp}(\Theta) = \frac{2\xi \cos\Theta \sin\Theta}{1-(\beta/2)P_2(\cos\Theta)} \tag{1}$$

$$A(\Theta) = \gamma \frac{A - \alpha P_2(\cos\Theta)}{1-(\beta/2)P_2(\cos\Theta)}. \tag{2}$$

Here, $P_2(\cos\Theta)$ is the second Legendre polynomial and γ denotes the light helicity. (Lefebvre-Brion and co-workers use the notation $\bar{P}$, ξ and γ for the spin polarization parameters (Raseev *et al* 1987).)

The spin polarization parameters A and ξ were determined either at the magic angle, $\Theta_{mag} = 54.74°$, where $P_2(\cos\Theta_{mag}) = 0$ or they are obtained from a least-squares fit of $A(\Theta)$ and $P_{\perp}(\Theta)$ angular distributions together with the parameters α and β. The photoelectrons corresponding to the $^2\Pi_{3/2}(v=1)$ vibrationally excited level and to the $^2\Pi_{1/2}(v=0)$ ground state have nearly equal kinetic energies (Delwiche *et al* 1972/73). Their influence on the experimental intensity and spin polarization results of the $^2\Pi_{1/2}(v=0)$ state was taken into account for the error estimations.

The photoelectron spectra were normalized by correcting for small changes in the target gas pressure, for the decrease of the photon flux and for the transmission characteristics of the electron spectrometer. The pressure in the experimental chamber was kept below 0.02 Pa. The absolute cross section scale (~20% error) was established by matching our intensity data to the results of Carlson *et al* (1984) at $E_{Photon} = 20$ eV (Salzmann *et al* 1994).

3. Results and discussion

The relative photoelectron intensity data taken at photon energies corresponding to the intensity peaks of several vibrational levels of the Rydberg resonances with an A $^2\Sigma^+$ core are shown in figure 2. All photoelectron spectra recorded in this energy region contain higher vibrational levels of the $^2\Pi$ states populated via the autoionizing Rydberg states. Due to the experimental energy resolution of $\Delta E_{FWHM} = 80$ meV and the small energy difference of the spin–orbit splitting and the vibrational constant (~330 meV and ~303 meV, respectively), the vibrational structure of the two $^2\Pi$ ionic states could not be completely separated, since for the lower vibrational levels the contributions from the states $^2\Pi_{3/2}(v=m+1)$ are superimposed on those from $^2\Pi_{1/2}(v=m)$. In particular, photoelectrons corresponding to the $^2\Pi_{1/2}(v=0)$ and $^2\Pi_{3/2}(v=1)$ final ionic states have nearly the same kinetic energy (Delwiche *et al* 1972/73) and could not be separated. This is the main reason for the different intensities of the two spin–orbit components of the $^2\Pi(v=0)$ level in the energy region examined (see also σ in figure 3).

The photoelectron spectra of figure 2 differ from the spectra usually observed outside the resonance region (Delwiche *et al* 1972/73, Yencha *et al* 1991) by the appearance of highly vibrationally excited peaks. To our knowledge, such photoelectron spectra with high vibrational excitation of the HBr^+ $^2\Pi$ final ionic states have not been reported before. There are close analogies to the spectra obtained for the corresponding energy region of the hydrogen halides HCl (Cafolla *et al* 1988) and HI (Böwering *et al* 1992a). The population of these vibrationally excited states can be attributed entirely to the influence of vibrationally excited autoionization resonances.

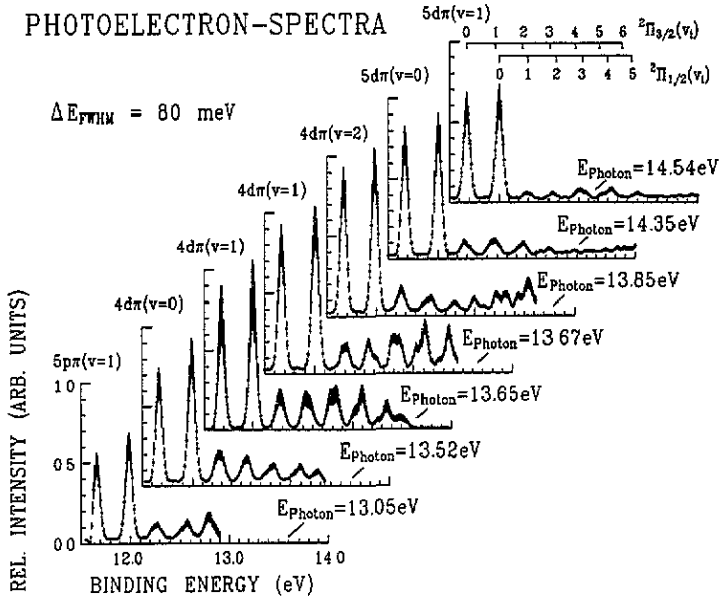

Figure 2. Photoelectron spectra for photon energies corresponding to different vibrational levels of the $np\pi$ and $nd\pi$ Rydberg states with an $^2\Sigma^+$ ionic core of HBr^+ (assignments taken from Lefebvre-Brion *et al* 1989).

The resonant spectra (figure 2) reflect the FCP in several ways. For direct ionization, there is only one prominent Franck-Condon factor (FCF) (see table 1(*a*)) and the two $^2\Pi(v=0)$ spin-orbit components are the strongest peaks. The population of the excited vibrational $^2\Pi(v=0)$ levels is primarily described by the product of two FCFs given in table 1(*b*) and 1(*c*), provided that the electronic transition moment is energy independent in this region (see also Terwilliger and Smith 1975):

$$|\langle HBr^+\,{}^2\Sigma^+\,v'|HBr\,{}^1\Sigma^+ v''=0\rangle|^2 * |\langle HBr^+\,{}^2\Pi\,v|HBr^+\,{}^2\Sigma^+\,v'\rangle|^2.$$

As a result of these FCF products (see table 2) for $v=0$ Rydberg states with an $A\,{}^2\Sigma^+$ core the $^2\Pi(v=1)$ and $(v=2)$, for the $v=1$ Rydberg states the $^2\Pi(v=0)$ and $(v=4)$, and for the $v=2$ Rydberg states the $^2\Pi(v=0)$ and $(v=2)$ are the most intense vibrational levels. This behaviour of the FCF products is roughly reproduced in the photoelectron spectra. In particular, it can be seen that vibrationally excited Rydberg resonances lead to an increased intensity of higher vibrational levels of the $^2\Pi$ final ionic states.

The cross section σ, the intensity asymmetry parameter β and the spin polarization parameters A and ξ for photoelectrons corresponding to the $^2\Pi_{1/2}(v=0)$ and $^2\Pi_{3/2}(v=0)$ final ionic states are shown in figure 3(*a–d*) for the photon energy region from 12.7–14.7 eV. For a better comparison, the results for the parameters A and ξ for the final ionic state $^2\Pi_{3/2}(v=0)$ are plotted with inverted sign. According to the non-relativistic theory for Hund's case (*a*) the following relationships hold (Cherepkov 1981): $A_{1/2}=-A_{3/2}$, $\xi_{1/2}=-\xi_{3/2}$, $\beta_{1/2}=\beta_{3/2}$ and $\sigma_{1/2}=\sigma_{3/2}$. The dashed curves represent the MQDT calculations (Lefebvre-Brion *et al* 1989) of σ, A and β for the $^2\Pi_{1/2}$ state convoluted to our experimental energy resolutions. The experimental data for both spin-orbit states are plotted at the same photon energy (and not at the same kinetic energy), since the influence of the Rydberg resonances on the photoionization process is large in the electronic autoionization region.

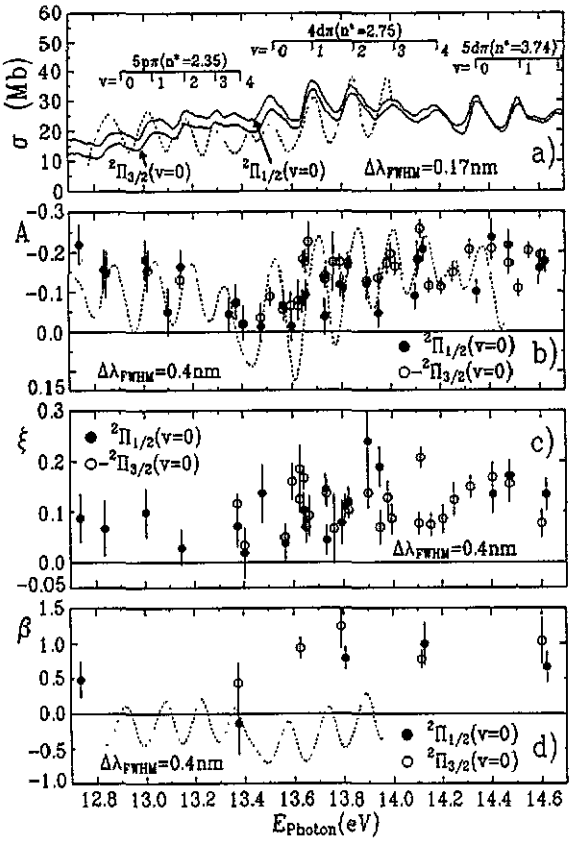

Figure 3. Absolute photoionization cross section σ (*a*), spin polarization parameters A (*b*) and ξ (*c*) and photoelectron angular distribution parameter β (*d*) for the $^2\Pi_{3/2}(v=0)$ and $^2\Pi_{1/2}(v=0)$ final ionic states of HBr^+. The dashed lines are results of a MQDT calculation (Lefebvre-Brion *et al* 1989) convoluted to the experimental resolution. Assignments are due to Lefebvre-Brion *et al* (1989) and Terwilliger and Smith (1975). The data points for the A and ξ values of the $^2\Pi_{3/2}(v=0)$ state are plotted with inverted sign. The calculated cross section is divided by 3.

The photoionization cross sections σ for the $^2\Pi$ states of HBr^+ (figure 3(*a*)) exhibit the vibrational structure of the A $^2\Sigma^+$ ion core of the Rydberg resonances for vibrational levels up to $v=3$. Higher vibrational levels are partially predissociated due to crossings with the repulsive $^3\Sigma_1^+$ and $^3\Pi_0$ states (Lefebvre-Brion *et al* 1989). In the corresponding energy region of the HI molecule the vibrational structure of the autoionization resonances is completely broadened (Böwering *et al* 1991). The calculated cross section σ for the $^2\Pi_{1/2}(v=0)$ state (figure 3(*a*)) is about three times larger and exhibits more pronounced oscillations of the Rydberg resonances than observed in the experimental results. The energetic positions for the 4dπ resonances agree with the experimental data, whereas for the 5pπ resonances a small energy shift is visible. The Rydberg resonance structures of earlier experimental relative photoionization cross sections (Dehmer and Chupka 1978) for the $^2\Pi$ state ($\Delta\lambda_{FWHM}=0.015$ nm, vibrationally averaged total ionization yield) are very similar to our results. This suggests that the widths of the Rydberg resonances are broadened due to the influence of predissociation as for HI (Böwering *et al* 1992b) and not limited substantially by our experimental resolution

Table 1. Franck–Condon factors (FCFs) $|\langle v'|v''\rangle^2|$: FCF's are calculated by solving the Schrödinger equation (Numerov 1933, Cooley 1961) with Morse-potential curves. The constants used are taken from Huber and Herzberg (1979). The results presented here are in good agreement with results for some of these FCFs obtained by Lefebvre-Brion *et al* (1989) and Banichevich *et al* (1992). Only the digits of interest are reported.

(*a*) $HBr\ ^1\Sigma^+\|v''\rangle \rightarrow HBr^+\ ^2\Pi\langle v'|$:						
v':	0	1	2	3	4	5
$v''=0$:	0.95	0.05	0.00	0.00	0.00	0.00
(*b*) $HBr^+\ ^2\Sigma^+\|v''\rangle \rightarrow HBr^+\ ^2\Pi\langle v'|$:						
v':	0	1	2	3	4	5
$v''=0$:	0.21	0.28	0.22	0.14	0.08	0.04
$v''=1$:	0.35	0.07	0.01	0.08	0.13	0.12
$v''=2$:	0.27	0.03	0.15	0.06	0.00	0.02
$v''=3$:	0.13	0.22	0.03	0.04	0.10	0.05
$v''=4$:	0.04	0.24	0.06	0.12	0.00	0.03
$v''=5$:	0.01	0.12	0.15	0.23	0.00	0.09
(*c*) $HBr\ ^1\Sigma^+\|v''\rangle \rightarrow HBr^+\ ^2\Sigma^+\langle v'|$:						
v':	0	1	2	3	4	5
$v''=0$:	0.11	0.26	0.29	0.20	0.09	0.03

Table 2. Products of Franck–Condon factors for a transition from the ground state HBr $^1\Sigma^+(v''=0)$ via Rydberg resonances with a $HBr^+\ ^2\Sigma^+$ v' ion core to vibrational levels of the $HBr^+\ ^2\Pi$ v final ionic states.

$\|HBr^+\ ^2\Sigma^+\ v'\|HBr\ ^1\Sigma^+\ v''=0\rangle\|^2 * \|\langle HBr^+\ ^2\Pi\ v\|HBr^+\ ^2\Sigma^+\ v'\rangle\|^2$						
v:	0	1	2	3	4	5
$v'=0$:	0.023	0.031	0.033	0.015	0.009	0.004
$v'=1$:	0.091	0.018	0.003	0.021	0.034	0.031
$v'=2$:	0.078	0.009	0.044	0.017	0.000	0.006

(the bandwidth of σ in this work is $\Delta\lambda_{FWHM}=0.17$ nm). The experimental relative photoabsorption cross section of Terwilliger and Smith (1975), obtained with an energy resolution of $\Delta\lambda_{FWHM}=0.02$ nm, is similar to the results presented here and displays only a slightly more pronounced vibrational structure. The differences between the photoionization and photoabsorption cross section structures are an indication for significant contributions from predissociation processes, which seem to have a larger influence on the $5p\pi$ than on the $4d\pi$ and $5d\pi$ Rydberg states (see figure 3(*a*)). The sum of the cross section for the two $^2\Pi(v=0)$ components determined at $E_{Photon}=14$ eV from our data ($\sigma=59.1\pm6.2$ Mb) agrees with the experimental result ($\sigma=58.8\pm9.0$ Mb) of Carlson *et al* (1984).

The spin polarization parameter A (figure 3(*b*)) displays a structure due to the oscillations of the σ^λ ($\lambda=\sigma, \pi, \delta$) partial cross section contributions caused by the Rydberg autoionization resonances (Lefebvre-Brion *et al* 1989). Many of the data points are in good agreement with the calculation if the uncertainty of the energy scale in the region examined is taken into account ($\Delta E<8.7$ meV). However, the theoretically predicted change of the sign of the spin polarization parameter A was not observed experimentally. To make sure that the bandwidth of the synchrotron radiation ($\Delta\lambda_{FWHM}=0.4$ nm) has no influence on the experimental A values, measurements with bandwidths of $\Delta\lambda_{FWHM}=0.25$ nm and $\Delta\lambda_{FWHM}=0.17$ nm were also performed at photon energies where a change of the sign for the parameter A was theoretically predicted. However, the A values obtained were found to be independent of the bandwidth of the

incident light within the experimental error. As a general trend, it may be noted that the oscillatory energy dependence for both the cross section σ and the spin polarization parameter A is more pronounced in the calculation than experimentally observed. The most distinct deviations between the theoretical and experimental A values exist in the energy region of the $4d\pi$ Rydberg resonance between the ($v=0$) and ($v=1$) levels as well as between the ($v=1$) and ($v=2$) levels. The deviations between the calculated and observed oscillations of the cross section σ in the $4d\pi$ energy region could also be the reason for the disagreement found between the theoretical and experimental values of the parameter A, since A and σ depend on the partial wave contributions σ^λ according to the equations (Raseev *et al* 1987):

$$\sigma = \sigma^\sigma + \sigma^\pi + \sigma^\delta$$
$$A_{1/2} = \tfrac{1}{2}\frac{\sigma^\sigma - \sigma^\delta}{\sigma^\sigma + \sigma^\pi + \sigma^\delta}. \tag{3}$$

According to equations (3), strong oscillations of the calculated values for either the σ^σ or the σ^δ partial cross section contributions can result in large oscillations for both σ and A.

The results for the ξ parameter for HBr^+ (figure 3(*c*)) indicate also pronounced oscillations in the region of the $4d\pi$ Rydberg states. This implies a strong energy dependence of the phases of the dipole matrix elements involved due to the large influence of the phase difference on the ξ parameter (Cherepkov 1981). The ξ values are small in the $5p\sigma$ and $5p\pi$ region, larger in the $4d\pi$ and $5d\pi$ region and drop again to small values in the energy region corresponding to the $6p\sigma$ and $6p\pi$ resonances near 14.2 eV (for resonance locations, see Terwilliger and Smith 1974, 1975).

The experimental data for the β parameter are less densely spaced, because they were obtained from measurements of the angular distributions according to equations (1) and (2). The calculated curve for the β parameter is based on the results reported previously (Lefebvre-Brion *et al* 1989). The deviations between theoretical and experimental results for the β parameter (figure 3(*d*)) are remarkable in the photoionization region considered. Except at $E_{\text{Photon}} = 13.38$ eV the experimental data for β show other values than theoretically predicted. Carlson *et al* (1984) obtained $\beta = 0.48 \pm 0.07$ at $E_{\text{Photon}} = 14$ eV for the unresolved $^2\Pi(v=0)$ states.

The β parameter for diatomic molecules depends on both the relative amplitudes of the dipole matrix elements and on the cosine of phase differences (Cherepkov 1981), whereas the A parameter depends only on the squares of the matrix elements. The small deviation of A and the strong disagreement of β between theory and experiment could be an indication of an incorrect description of the phases of the matrix elements in the calculation. The phases should have an oscillatory energy dependence as the values obtained for the ξ parameter suggest.

Combinations of the cross sections σ and the A parameters, according to equations (3), allow a determination of partial cross section sums (Böwering *et al* 1992b):

$$\sigma(\delta, \pi) = \sigma^\delta + \sigma^\pi/2 = (0.5 \pm A)\sigma$$
$$\sigma(\sigma, \pi) = \sigma^\sigma + \sigma^\pi/2 = (0.5 \mp A)\sigma. \tag{4}$$

The upper sign refers to a $^2\Pi_{3/2}$, the lower to a $^2\Pi_{1/2}$ ionic state. Thus, application of the equations (4) to the experimental results enables a further partitioning of the partial cross sections. Sums of partial cross section contributions $\sigma(\lambda, \pi)$ ($\lambda = \sigma, \delta$) are shown

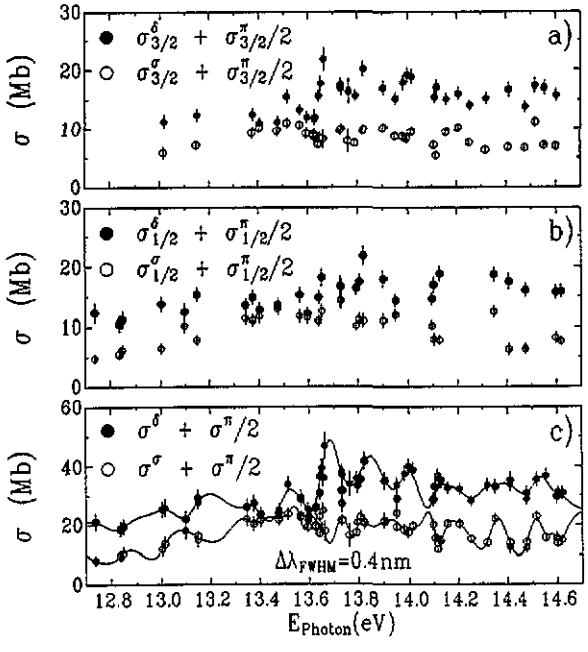

Figure 4. Absolute partial cross section sums $\sigma^{\delta}+\sigma^{\pi}/2$ and $\sigma^{\sigma}+\sigma^{\pi}/2$ for the final ionic states of HBr^{+} $^{2}\Pi_{3/2}(v=0)$ (*a*) and $^{2}\Pi_{1/2}(v=0)$ (*b*) separately and for their sum (*c*). The solid lines are results of a tensioned spline fit to the data for a better illustration of the resonance structures.

separately for the $^{2}\Pi_{3/2}(v=0)$ and $^{2}\Pi_{1/2}(v=0)$ ionic states in figure 4(*a*) and (*b*). To obtain a higher data point density the sum of the cross sections for the two HBr^{+} $^{2}\Pi(v=0)$ states was combined with the experimental values for $A_{3/2}$ and $A_{1/2}$, respectively. These results are shown in figure 4(*c*). The solid line in figure 4(*c*) is a result of a smoothed tensioned spline fit (Späth 1986) for a better illustration of the oscillations of $\sigma(\sigma, \pi)$ and $\sigma(\delta, \pi)$. An even higher density of the data points in the resonance region examined in figures 3 and 4 would be desirable. Unfortunately, due to the required time-consuming Mott analysis, apart from the data for σ, the experimental results still contain gaps and are not sufficiently dense to give a complete account of the energy dependence of the dynamical parameters. However, the major features of the resonant photoionization can be discerned even with the limited amount of data available. Figures 4(*a–c*) reflect large oscillating σ^{δ} contributions to the total cross section σ, whereas the σ^{σ} contributions have always a smaller magnitude and more weakly oscillating structures as compared to σ^{δ}. The most pronounced σ^{δ} contributions are in the range of the $4d\pi$ Rydberg states. The experimentally and theoretically obtained σ and A values were used for a comparison between the ratios of the determined $\sigma(\sigma, \pi)$ and $\sigma(\delta, \pi)$ partial cross sections. The comparison of the relative contributions of σ^{σ} to the total cross section σ shows that the results obtained from the theoretical values are always larger.

For further discussion it is of interest to compare the experimental results of figure 3 and figure 4 for the $(np\pi)^{3}\,^{2}\Pi$ final ionic states of HBr^{+} ($n=4$) with those of HI^{+} ($n=5$) (Böwering *et al* 1991, 1992b) for the corresponding energy region, since both molecules have similar molecular orbital structure. The oscillations of the A parameter

observed for HBr^+ were not obtained in the case of HI^+, due to the strong broadening of the Rydberg resonances of HI by predissociation processes. A change of the sign of A in the resonance region, theoretically predicted for HBr^+, was not observed experimentally for both molecules. However, apart from strong oscillations of the A parameters of HBr^+ in the energy region examined a similar general energy dependence can be seen as for HI^+. The A values for the two $^2\Pi(v=0)$ final ionic states of HI^+ (Böwering *et al* 1991) exhibit a broad decrease to almost zero in the range of the $6p\pi$ Rydberg states, an increase to maximal values in the range of the $5d\pi$ Rydberg states and have a drop to small polarization values at higher photon energies, directly above the $5d\pi$ state. For HBr, larger values are observed in the range of the $4d\pi$ and $5d\pi$ Rydberg resonances whereas many of the A values in the range between 13.3 eV and 13.6 eV are very small. This corresponds exactly to the energy region where the calculation (Lefebvre-Brion *et al* 1989) for HBr^+ predicts predissociation to occur via the $4d\sigma$ $^1\Sigma^+$ state. The influence of these predissociating resonances which give rise to outgoing $\varepsilon l\pi$ waves could be the reason for the decrease of the spin polarization in the region of 13.3 eV to 13.6 eV. (According to equations (3), the polarization parameter A decreases if the σ^π partial contribution increases.) These similarities for HBr and HI molecules suggest a typical behaviour for A around the $4d\pi$ (HBr) and $5d\pi$ (HI) Rydberg resonances, respectively. In the energy region below about 14.3 eV a less pronounced drop to smaller values of the parameter A is observed. These pronounced dips affecting both the σ and A parameters could be connected to the rather small FCF for the vibrational transition $HBr^+\ ^2\Sigma^+|v'=4\rangle \rightarrow HBr^+\ ^2\Pi\langle v''=0|$ compared to the large FCF for $HBr^+\ ^2\Sigma^+|v'=4\rangle \rightarrow HBr^+\ ^2\Pi\langle v''=1|$ (see table 1(*b*)). This would result in a decrease of the contribution via autoionizing Rydberg states for the $HBr^+\ ^2\Pi(v=0)$ partial cross section with a related influence on the connected photoionization parameters, which depends on the FCF.

The determined values of $\sigma(\sigma, \pi)$ and $\sigma(\delta, \pi)$ for the two $\Pi(v=0)$ final ionic states of HI^+ (Böwering *et al* 1992b) exhibit in the corresponding energy region only a weak energy dependence for the $\sigma(\sigma, \pi)$ cross section, whereas $\sigma(\delta, \pi)$ which is always larger than $\sigma(\sigma, \pi)$ has a broad resonance structure in the range of the $5d\pi$ Rydberg states, due to a rise and decrease of the σ^δ contributions. Above all, for HBr and HI (Böwering *et al* 1992b) the contributions of the σ^σ and σ^δ partial cross sections dominate the total cross section σ for ionization with electron emission from the outermost $p\pi$ orbital of the ground state, due to the atomic-like dipole selection rule $\Delta\lambda = 1$, and σ^δ is always the largest. The contribution of the partial cross section σ^π to σ should be very small, with the exception of the region from 13.3 eV–13.6 eV, where the polarization values for the A parameter were found to be close to zero.

4. Conclusions

The A and ξ spin polarization parameters, as well as the cross sections σ and σ^λ for HBr exhibit in the energy range close to the Rydberg resonances characteristic energy dependences due to autoionization and predissociation processes and to the FCP. The influence of the intermediate resonance states is also strongly visible in photoelectron spectra taken in the resonance region, which show population of high vibrational levels.

The dominant σ^σ and σ^δ partial cross section contributions determined from partial cross section sums $\sigma(\lambda, \pi)$ ($\lambda = \sigma, \delta$) of HBr and HI (Böwering *et al* 1992b) illustrate the basic atomic-like behaviour of the photoionization of the HBr and HI (Böwering

et al 1991, Raseev *et al* 1987) molecules with strong additional influences of autoionization and predissociation processes. This atomic-like behaviour could be caused by the weak influence of the light hydrogen atom on the molecule compared to the heavy halogen atom which dominates the photoionization dynamics.

A fair agreement between the experimental results and the theoretical treatment of HBr^+ is obtained for the parameters σ and A (Lefebvre-Brion *et al* 1989). In particular, the predicted and measured oscillation structures of the σ and A parameters are found to agree reasonably well, if the less pronounced behaviour of the experimental values for σ and A is taken into account. The stronger oscillatory structure in the calculation for the cross section σ and the A parameter compared to the experimental data could be an indication that the influences of predissociating states are underestimated in the theory. Especially, the transfer of the results of a theoretical treatment on HCl (Lefebvre-Brion and Keller 1989) concerning the predissociated states to HBr—the $^1\Pi$ Rydberg states should be autoionized and the $^1\Sigma^+$ Rydberg states should be preferentially predissociated—could be the reason for the disagreement observed between theoretical and experimental data. A recent theoretical treatment of predissociation processes of the excited A $^2\Sigma^+$ state of HBr^+ (Banichevich *et al* 1992) shows, that all repulsive $^4\Sigma^-$, $^2\Sigma^-$ and $^4\Pi$ states are involved in these processes. The transfer of this result to the electronic autoionization region predicts predissociation of the $^1\Pi$ as well as the $^1\Sigma^+$ Rydberg states, caused by the repulsive $^3\Sigma_1^+$ and $^3\Pi_0$ Rydberg states. Under this condition the reasons for the more pronounced calculated oscillations of σ and A in comparison with the experiment are the stronger predissociation of the $^1\Pi$ Rydberg states by respulsive states or several neglected interactions between repulsive and non-repulsive Rydberg states. The strong energy dependence of the phase differences of the matrix elements in this energy region, obtained from the experimental ξ parameters, suggests that the theoretical modelling of the phases is not sufficiently accurate. This affects also the calculated values for the β parameter. Theoretical and experimental results of the σ, A, ξ and β parameter for higher vibrational levels would be helpful so that the intrachannel coupling between different vibrational levels could be analysed.

Acknowledgments

The authors thank H Lefebvre-Brion for many illuminating discussions and for making available her calculations for the σ, A and β parameters. We would also like to thank M Müller for his assistance in the measurements of the A parameter and acknowledge the support by the BESSY staff. This work was supported by BMFT under contract 055PBAXI.

References

Adam M Y, Keane M P, Naves de Brito A, Correia N, Baltzer P, Wannberg B, Karlsson L, Svensson S 1992 *J. Electron Spectrosc. Relat. Phenom.* **58** 185–97

Ballard R E 1978 *Photoelectron Spectroscopy and Molecular Orbital Theory* (Bristol: Adam Hilger)

Banichevich A, Klotz R and Peyerimhoff S D 1992 *Mol. Phys.* **75** 173–88

Böwering N, Klausing H-W, Müller M, Salzmann M and Heinzmann U 1992a *Chem. Phys. Lett.* **189** 467–72

Böwering N, Salzmann M, Müller M and Heinzmann U 1991 *J. Phys. B: Mol. Opt. Phys.* **24** 4793–801

Böwering N, Salzmann M, Müller M, Klausing H-W and Heinzmann U 1992b *Phys. Rev.* A **45** R11–45

Cafolla A A, Comer J and Reddish T 1988 *J. Phys. B: At. Mol. Opt. Phys.* **21** 3571–84

Carlson Th A, Fahlman A, Krause M O, Whitley T A and Grimm F A 1984 *J. Chem. Phys.* **81** 5389–94
Cherepkov N A 1981 *J. Phys. B: At. Mol. Phys.* **14** 2165–77
Cooley J W 1961 *Math. Comput.* **15** 363–79
Dehmer P M and Chupka W A 1978 *Argonne National Laboratory Report ANL-78-65* part I, pp 13–8
Delwiche J, Natalis P, Momigny J and Collin J E 1972/73 *J. Electron Spectrosc.* **1** 219–25
Heckenkamp Ch, Schäfers F, Schönhense G and Heinzmann U 1984 *Phys. Rev. Lett.* **52** 421–4
—— 1986 *Z. Phys.* D **2** 257–74
Huber K P and Herzberg G 1979 *Molecular Spectra and Molecular Structure Vol IV Constants of Diatomic Molecules* (New York: Van Nostrand-Reinhold)
Jost K 1979 *J. Phys. E: Sci. Instrum.* **12** 1006–12
Lefebvre-Brion H, Dehmer P M and Chupka W A 1988 *J. Chem. Phys.* **88** 811–7
Lefebvre-Brion H and Keller F 1989 *J. Chem. Phys.* **90** 7176–83
Lefebvre-Brion H, Salzmann M, Klausing H-W, Müller M, Böwering N and Heinzmann U 1989 *J. Phys. B: Mol. Opt. Phys.* **22** 3891–900
Lempka H J, Passmore T R and Price W C 1968 *Proc. R. Soc.* A **304** 53
Numerov B 1933 *Publ. Obs. Centr. Astrophys. Russ.* **2** 188–201
Raseev G, Keller F and Lefebvre-Brion H 1987 *Phys. Rev.* A **36** 4759–74
Salzmann M, Böwering N, Klausing H-W and Heinzmann U 1994 to be published
Schäfers F, Peatman W, Eyers A, Heckenkamp Ch, Schönhense G and Heinzmann U 1986 *Rev. Sci. Instrum.* **57** 1032–41
Späth H 1986 *Spline-Algorithmen* 4th edn (München: Oldenbourg)
Terwilliger T D and Smith A L 1974 *J. Mol. Spectrosc.* **50** 30–7
—— 1975 *J. Chem. Phys.* **63** 1008–20
Yencha A J, Ruf M-W and Hotop H 1991 *Z. Phys.* D **21** 113–30